Macromolecules
ARTICLE

Macromolecules **2010**, *43*, 1129–1136 **1129**
DOI: 10.1021/ma902325b

Effective Charge of Adsorbed Poly(amido amine) Dendrimers: Transition from Heterogeneous to Homogeneous Charge Distribution

Ionel Popa,[†] Georg Papastavrou,[‡] and Michal Borkovec*

Department of Inorganic, Analytical, and Applied Chemistry, University of Geneva, Sciences II, 30, Quai Ernest-Ansermet, CH-1211 Geneva 4, Switzerland. [†]On leave to: Department of Biological Sciences, Columbia University, New York, 10027. [‡]Current address: Physical Chemistry II, University of Bayreuth, D-95440 Bayreuth, Germany

Received October 19, 2009; Revised Manuscript Received November 19, 2009

ABSTRACT: The surface charge density of sulfate latex particles with adsorbed poly(amido amine) (PAMAM) dendrimers of generation 10 was determined from direct force measurements with atomic force microscopy (AFM). The variation of the surface charge density with the adsorbed amount can be related to the effective charge of the dendrimers in the adsorbed state. Two regimes were identified. In the first regime, the adsorbed amount is low and the surface charge distribution strongly heterogeneous. This regime is characterized by an effective charge of about 45 elementary charges. The second regime corresponds to a saturated layer with higher adsorbed amount and a more homogeneous charge distribution. This regime is characterized by a higher effective charge of about 93, which is comparable to the value expected from Poisson−Boltzmann theory. The transition between these two regimes is located in a narrow region just after the charge reversal point.

1. Introduction

The control of colloidal suspension stability is essential in many industrial applications.[1−6] The destabilization of such suspensions is important in papermaking or wastewater treatment, whereby rapid aggregation of the suspension in question is necessary.[2,3] On the other hand, suspension stabilization is essential in order to achieve long shelf life of consumer products, such as cosmetics, foods, or drugs.[4,5]

Oppositely charged polyelectrolytes are frequently used as additives to control the stability of such suspensions.[2,5,7−12] These polyelectrolytes adsorb strongly to the surfaces of colloidal particles, whereby they influence the surface charge, interaction forces, and consequently the suspension stability. Several authors have demonstrated that addition of oppositely charged polyelectrolytes initially leads to charge neutralization and subsequent charge reversal (i.e., overcharging).[7−12] The charge reversal is determined by the adsorption process of the polyelectrolyte. The interaction forces and the resulting colloid stability can be qualitatively explained by the classical theory of Derjaguin, Landau, Verwey, and Overbeek (DLVO).[6,13,14] This theory stipulates that the interactions are governed by repulsive forces due to overlap of diffuse layers and attractive van der Waals forces. However, additional attractive forces seem to be present in such systems, and they originate most likely from the laterally uneven patch-charge distributions.[1,7]

To better understand the role of polyelectrolyte branching, researchers have investigated the adsorption of cationic dendrimers and their capability to modify interaction forces as well as colloidal stability.[15−22] The most frequently studied systems involve poly(amino amide) (PAMAM) dendrimers.[23−27] They are positively charged in aqueous solutions and available up to generation 10 (G10). These dendrimers were shown to influence the stability of negatively charged particle suspensions similarly to cationic polyelectrolytes.[1,15,17] At the same time, they are relatively monodisperse and can be easily imaged and counted on surfaces with the atomic force microscope (AFM).[19,28,29] For these reasons, PAMAM dendrimers are an ideal model system to study the influence of branched polyelectrolytes on colloidal interactions.

While colloidal stability is determined by the interaction forces between particles, detailed information on these forces is difficult to obtain from stability measurements. More recently, direct force measurements made possible to access the actual force profiles determining the interactions in question. In many situations, interactions were studied between mica sheets with the surface forces apparatus,[30,31] or between particles and surfaces with the AFM-based colloidal probe and related techniques.[32−36] Such studies have demonstrated that interactions between surfaces with adsorbed polyelectrolytes are indeed DLVO-like, and that additional attractive forces stronger than van der Waals forces are present. However, direct force measurements were mostly carried out at high polyelectrolyte dose, and the interesting regime close to the charge reversal point could be accessed only with difficulties.

Several studies have attempted to rationalize the strength of the electrostatic repulsive forces between adsorbed polyelectrolyte layers due to diffuse layer overlap.[30,32,33,35−38] These forces are related to the surface charge density compensating the diffuse layer charge. This charge turns out to be substantially lower than the bare (or stoichiometric) charge of the adsorbed polyelectrolyte. Various experimental studies suggest that mere 5−10% of the polyelectrolyte charge is neutralized by the diffuse layer.[36,38] The remaining part is neutralized by coadsorbed counterions of the polyelectrolyte. From direct force measurements between silica surfaces in the presence of PAMAM dendrimers, it was possible to obtain estimates of effective charges of the adsorbed dendrimers.[37] These charges are about 100 times smaller than the bare charges. These values are in good agreement with

*To whom correspondence should be addressed. E-mail: michal.borkovec@unige.ch. Telephone: 0041 22 379 6405.

Published on Web 12/03/2009

Poisson−Boltzmann theory for charged spherical objects in electrolyte solutions.[39,40] The effective charge is an important parameter, as it can be used to predict the diffuse layer potential controlling the repulsive forces and consequently the suspension stability.

The present study reports direct force measurements between individual colloidal latex particles with the AFM in the presence of PAMAM G10 dendrimers. The presently used multiparticle colloidal probe technique has two major advantages over most approaches reported so far. First, the colloidal particles are attached to the cantilever and the substrate in the electrolyte solution, thus avoiding the problematic drying-rewetting step, which often leads to the formation of nanosized bubbles on latex particles. Second, the internal surface area in the colloidal suspension used is very high, making the control of the polyelectrolyte dose straightforward. These two advantages open the possibility to obtain accurate force profiles over the whole range of adsorbed amount, especially near the charge reversal point. This article discusses the repulsive part due to diffuse layer overlap in detail and reanalyzes the concept of the effective charge to predict the diffuse layer potential. In a previous letter, direct force measurements on the same system close to the charge reversal point were compared with computer simulations.[41]

2. Experimental Section

Materials. The PAMAM G10 dendrimers from Dendritech (Midland, MI) were used without further purification. For perfect dendrimers, one expects a molecular mass of 935 kg/mol and 8190 ionizable amine groups. Because of the incomplete yield of the reaction steps during synthesis, dendrimers tend to have lower molecular mass and finite polydispersity.[42,43] A polydispersity index of about 1.3 was reported, and this number might vary from batch to batch.[26,28,29] The hydrodynamic radius of 6.8 nm was obtained by dynamic light scattering. At pH 4, essentially all amine groups are charged.[25] Negatively charged polystyrene latex particles with sulfate surface groups were purchased from Interfacial Dynamics Corporation (IDC, Portland, OR). The manufacturer reports a particle diameter of 3.1 μm and a polydispersity of 5.6% obtained with transmission electron microscopy, and a surface charge density of −67 mC/m^2 determined by conductivity. The particles were dialyzed for more than 6 h in a Millipore ultrafiltration apparatus. Concentrations of the particle suspensions and the dendrimer solutions were verified by total organic carbon and nitrogen analysis (TOC-V, Shimadzu). For routine analysis, particle concentrations were determined by light scattering by comparing the scattering intensity of an unknown sample with a reference sample of known concentration. Dilute HCl was used to adjust the solution pH 4, while the ionic strength was adjusted with KCl. Water purified with a Millipore Milli-Q system was used throughout.

AFM Imaging. A multimode Nanoscope IIIa (Vecco, Santa Barbara, CA) in tapping mode was used to image the latex particles. Dendrimer solutions were added to particle suspensions and left to react overnight. Subsequently, they were filtered with a membrane filter with pores of 1.2 μm (Isopore, Millipore). The filters were rinsed with water, dried in vacuum for few hours, and imaged in air in tapping-mode with standard silicon cantilevers (OMLC-AC160TS-W2, Olympus, Japan). A sphere-cap was fitted to the AFM image and the dendrimers were counted in a circular area at the top of each particle. Adsorbed number densities were estimated by counting the dendrimers for at least five particles. By invoking the known molecular mass, the adsorbed mass of the dendrimers was obtained. This quantity agreed well with the amount of dendrimers added to the suspension, confirming that the adsorption was quantitative below the saturation plateau. From the adsorbed number densities, the surface coverage was equally estimated by assuming the previously reported radius of 9.2 nm in the adsorbed state.[29]

Direct Force Measurements. A closed-loop AFM (MFP-3D, Asylum Research, Santa Barbara, CA) mounted on an inverted optical microscope (IX70, Olympus) was used to directly measure the forces between two colloidal particles. Piranha solution consisting of a mixture of H_2SO_4 98% and H_2O_2 30% in a ratio of 3:1 was used at 80 °C for 40 min to clean the glass plate fitting the fluid cell. After extensive rinsing with water, the plate was treated in a plasma cleaner (PDC-32G, Harrick, New York) for 20 min. This plate was finally silanized for 2 h over 3-(ethoxydimethylsilyl)propylamine (Sigma-Aldrich) under vacuum in an airtight container. The silanization was verified by assuring that the static contact angle of a water drop was larger than 30°. After a measurement, particles were removed from the glass plate with Hellmanex solution and the plate was rinsed in water. The tipless AFM cantilevers (MikroMasch, Tallinn, Estonia) were cleaned with air plasma for 20 min and silanized in the same way as the glass substrate.

Dendrimer solutions of concentrations around 1 mg/L were added to latex particle suspensions of approximate concentrations of 100 mg/L and were left to adsorb overnight in vacuum at pH 4 and appropriate ionic strength. Dendrimer adsorption was verified by measuring the electrophoretic mobility of the particles by video microscopy with ZetaCompact (CAD Instrumentation, Les Essarts le Roi, France).

After mounting the fluid cell, the particle suspension was injected and left to sediment for about 3 h in the fluid cell, whereby particles adsorbed to the glass plate. Subsequently, the electrolyte solution with pH 4 and the desired ionic strength was degassed in a Gasstor degasser for 1−2 h and injected in the AFM fluid cell. For the experiments with the saturated adsorbed layer, the ionic strengths used for adsorption and during the AFM measurement could be varied and were eventually different.

By pressing the silianized cantilever against an adsorbed particle in the fluid cell with the AFM and rolling it at the same time, it was possible to firmly attach this particle to the cantilever. This particle was centered over another adsorbed particle with a precision of about 0.3 μm by observing the interference fringes in the optical microscope. For each pair of particles, about 100 approach−retraction forces profiles were measured at a frequency of 0.5 Hz and an approach velocity of 400−800 nm/s and averaged. The particle was finally detached from the cantilever by pressing it against the substrate, and another particle was attached for a subsequent measurement. Forces between different pairs of particles could be measured with the same cantilever and in the same solution.

The forces were obtained from the cantilever deflection. The onset of the constant compliance region was used to determine the zero separation with a precision of about 0.2 nm. The spring constants of the cantilevers were in the range of 0.04 and 0.3 N/m. They were determined with three independent methods.[44−46] The respective values agreed within 20% and the average of these three values was used. The force was normalized to the effective radius given by $R_{eff} = R_1R_2/(R_1 + R_2)$ where R_1 and R_2 are the radii of the both interacting particles, as determined by optical microscopy with a precision of about 0.2 μm.

3. Results and Discussion

Forces between two individual colloidal particles were measured directly with an AFM in aqueous particle suspensions at pH 4 and various ionic strengths adjusted with KCl. The investigated particles are negatively charged sulfate latex particles, and their interaction forces were determined in the presence of adsorbed positively charged PAMAM G10 dendrimers and in their absence. From these measurements, the diffuse layer potential and the compensating charge density of the diffuse layer are calculated. By relating the latter quantity to the amount of

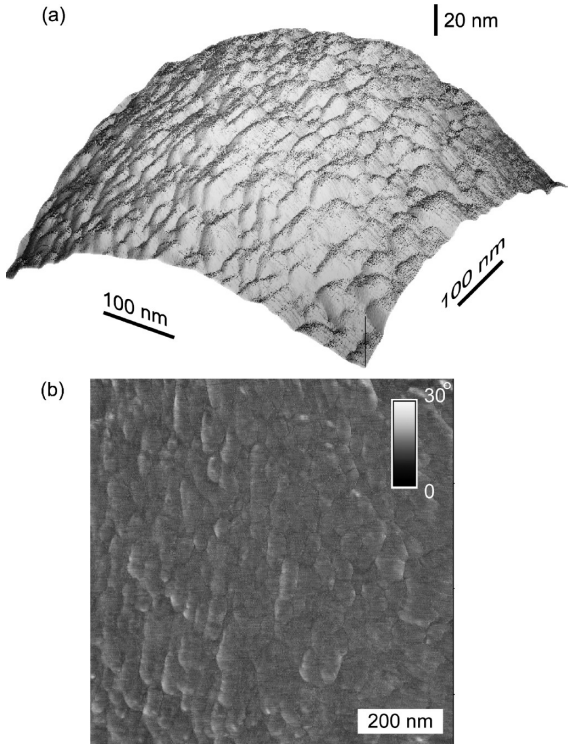

Figure 1. (a) AFM phase image of a bare latex particle and (b) the corresponding flattened image.

dendrimers adsorbed, information on the effective charge of the dendrimers in the adsorbed state is obtained. The presently used suspension technique permits precise control of the dendrimer dose and avoids drying of the latex particles during preparation.

Bare Latex Particles. Figure 1 shows AFM images of the sulfate latex particles in air. The flattened image indicates only small asperities. From topographic images one concludes that the particles are rather smooth with a mean square roughness of 1.3 nm. Direct force measurements were first carried out between these particles in the absence of dendrimers. Figure 2a shows the averaged approach force profiles at different ionic strengths. At larger distances, the measured forces decay exponentially. The characteristic decrease of the decay length with increasing ionic strength suggests that the interactions are of electrostatic nature and originate from the overlap of the diffuse layers. At smaller distances, the force profiles remain repulsive down to contact. At higher ionic strengths, attractive forces at short distances were observed. They originate most likely from van der Waals interactions. The absence of jump-ins indicates that the latex particle surfaces are free of spurious nanosized air bubbles.[47,48]

The solid lines in Figure 2a represent the fits to the numerical solution of the PB equation with constant regulation (CR) boundary condition.[49] The inset shows that this boundary condition typically leads to force profiles between the classical boundary conditions of constant charge (CC) and of constant potential (CP). Note that the latter condition does not represent a lower bound to the force.[50] From such fits of the force profiles, three parameters can be extracted, namely, the decay constant, the diffuse layer potential, and the regulation parameter. The decay constant is given by the inverse Debye length κ^{-1}, which can be expressed as

$$\kappa^2 = \frac{2e^2 N_A I}{\varepsilon\varepsilon_0 kT} \quad (1)$$

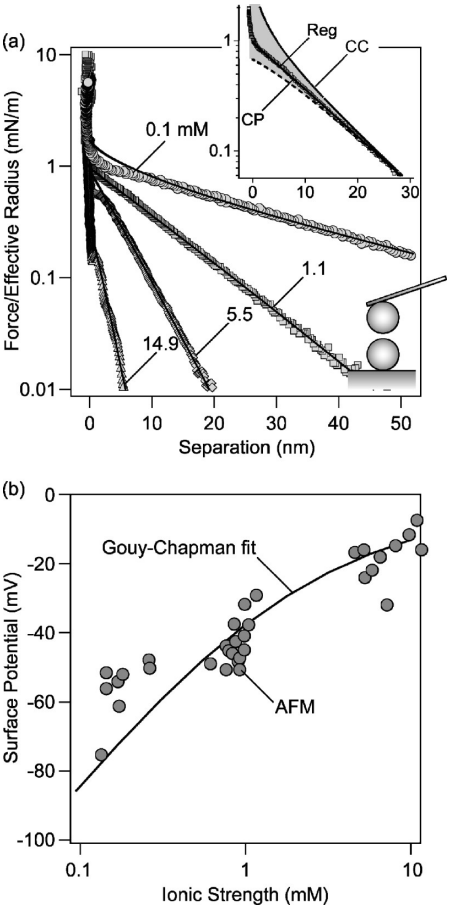

Figure 2. Interactions between sulfate latex particles in KCl electrolyte at pH 4. (a) Force profiles measured with the AFM as a function of the separation distance for different fitted ionic strengths with the fit to PB theory with constant regulation (CR) boundary condition. The insets show the scheme of the experiment and the corresponding results for the classical conditions of constant charge (CC) and constant potential (CP) boundary conditions. (b) Measured diffuse layer potentials obtained from the force profiles as a function of ionic strength fitted to the Gouy−Chapman relation. The resulting surface charge density is −3.0 mC/m^2.

where e is the elementary charge, N_A is the Avocadro's number, I the ionic strength, $\varepsilon\varepsilon_0$ the dielectric permittivity of water, k the Boltzmann constant, and T is the absolute temperature. The measured decay lengths always agreed within 15% with the expected Debye length calculated from the nominal ionic strength of the solution. The diffuse layer potential ψ_d determines the magnitude of the repulsive force. While the sign of the potential cannot be found from force measurements in symmetric systems, its negatively charged sign can be inferred from negative electrophoretic mobility of the particles, and the fact that the sulfate surface groups are negative at pH 4. The regulation parameter p ($p \leq 1$) characterizes the charge regulation process, whereby $p = 1$ corresponds to boundary conditions of CC and $p = 0$ to CP. The regulation parameter is $p = 0.3 \pm 0.2$ and features no clear trends with the ionic strength. This value indicates that charge regulation does take place.

Figure 2b shows that the magnitude of diffuse layer potential decreases with decreasing ionic strength. Within the PB theory, the diffuse layer potential is related to the surface charge through the Gouy−Chapman equation

$$\psi_d = \frac{2kT}{e}\,\mathrm{asinh}\left(\frac{e\sigma}{2kT\varepsilon\varepsilon_0\kappa}\right) \quad (2)$$

where σ is the surface charge density compensating the diffuse layer charge. Figure 2b shows that this relation describes the ionic strength dependence of the diffuse layer potential with a surface charge density of $\sigma = -3.0 \pm 0.3$ mC/m^2 rather well. However, the magnitude of this charge density is substantially smaller than the one obtained from conductivity. This discrepancy probably originates from specific adsorption of potassium ions to the latex particle surface.

Latex Particles with Adsorbed Dendrimers. Figure 3 shows an AFM image of a latex particle with adsorbed PAMAM G10 dendrimers. The flattened phase image confirms that the dendrimers adsorb to the latex particles individually in a loose monolayer. The same adsorption behavior was reported for planar silica substrates and mica.[28,29] For the latter substrates, the height of the dendrimers was reported 4.3 nm and their radius 9.2 nm, indicating that the dendrimers fatten strongly in the adsorbed state. This deformation due to strong attractive electrostatic interactions between the dendrimer and the substrate was discussed previously.[22,28,29,51,52] The adsorbed number density of the dendrimers on the surface is determined by counting the dendrimers in a circular area at the particle top, and by normalizing to the surface area of the corresponding spherecap. The dendrimers are adsorbed irreversibly on the latex particles, and they do not desorb in electrolyte solutions free of dendrimers at pH 4 over a period of several hours. This point can be verified by flushing the particles with a pure electrolyte solution, and counting the dendrimers again with the AFM. This finding is equally consistent with the fact that G10 dendrimers do not desorb from silica,[22] which has a charge density comparable to the latex particles used here.

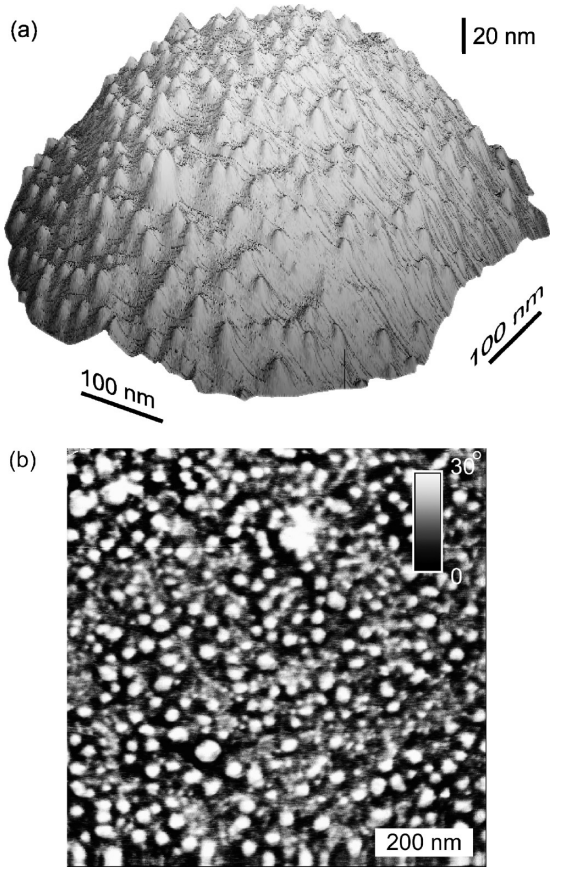

Figure 3. (a) AFM image of a latex particle covered with G10 dendrimers adsorbed in pH 4 and 1 mM KCl and (b) the corresponding flattened phase.

Direct force measurements were first carried out between the sulfate latex particles when dendrimers were adsorbed from a solution of a given ionic strength with dendrimers added in excess. Under such conditions, the adsorbed amount is controlled by the ionic strength of the electrolyte solution only, and we refer to a saturated layer. The corresponding adsorbed amount was obtained independently by counting the dendrimers in the AFM images and is given in Table 1. The adsorbed amount is quite similar to the one observed at pH 6 for PAMAM G10 dendrimers on silica.[19] The magnitude of the bare surface charge density of silica at this pH is somewhat lower than the corresponding value for the latex particles. The fact that the adsorbed amount is nevertheless comparable in both situations could be explained by the fact that the surface of polystyrene latex particles is more hydrophobic than the one of silica.

Figure 4 shows the resulting force profiles between saturated dendrimer layers. Note that the ionic strength used for the force measurement was eventually different from the one used during the adsorption conditions. However, since the dendrimer adsorption is irreversible, the amount of adsorbed dendrimers remains constant during the experiments. One observes that the force profiles are strongly repulsive at larger distances. At smaller distances, a short-ranged attractive component appears. This component is most pronounced at the lowest adsorbed amount of 1.41 mg/g, and vanishes at the highest one of 2.04 mg/g. The attractive forces originate probably from patch-charge interactions induced by the uneven charge distributions resulting from the positively charged dendrimers adsorbed on the negatively charged surfaces. Since the range of these interactions is dictated by the size of these heterogeneities,[53] one expects that the range decreases with increasing adsorbed amount. At the same time, the surface charge distribution becomes more homogeneous, leading to weaker attractive forces.

The repulsive parts of the force profiles were fitted to the PB model with CR boundary condition. The decay length agrees with the expected value from the nominal ionic strength of the solution within 15%. The regulation parameter $p = 0.4 \pm 0.1$ did not show any clear trends. The resulting diffuse layer potential is plotted as a function of the ionic strength in Figure 5. The fact that the diffuse layer is positive can be inferred from the fact that the magnitude of the surface potential increases with increasing adsorbed amount of the positively charged dendrimers. The observed dependence on the ionic strength can be well described with the Gouy−Chapman relation (eq 2). The applicability of this relation provides a further confirmation of the fact that the charge originating from the dendrimers does not vary with

Table 1. Properties of saturated layers of adsorbed G10 dendrimers on sulfate latex at pH 4

ionic strength[a] (mM)	adsorbed mass[b] (mg/g)	adsorbed mass[b] (mg/m^2)	number density[b] (μm^{-2})	coverage[b]	charge density[c] (mC/m^2)
0.1	1.41 ± 0.09	0.76 ± 0.05	496 ± 31	0.126 ± 0.008	4.2 ± 0.2
1.1	1.55 ± 0.06	0.84 ± 0.03	544 ± 22	0.138 ± 0.006	4.9 ± 0.2
10.1	2.04 ± 0.11	1.11 ± 0.06	716 ± 41	0.182 ± 0.010	8.1 ± 0.6

[a] Ionic strength during the adsorption process. [b] Obtained by counting of the dendrimers from AFM images. [c] From Gouy−Chapman relation applied to the surface potentials obtained by direct force measurements.

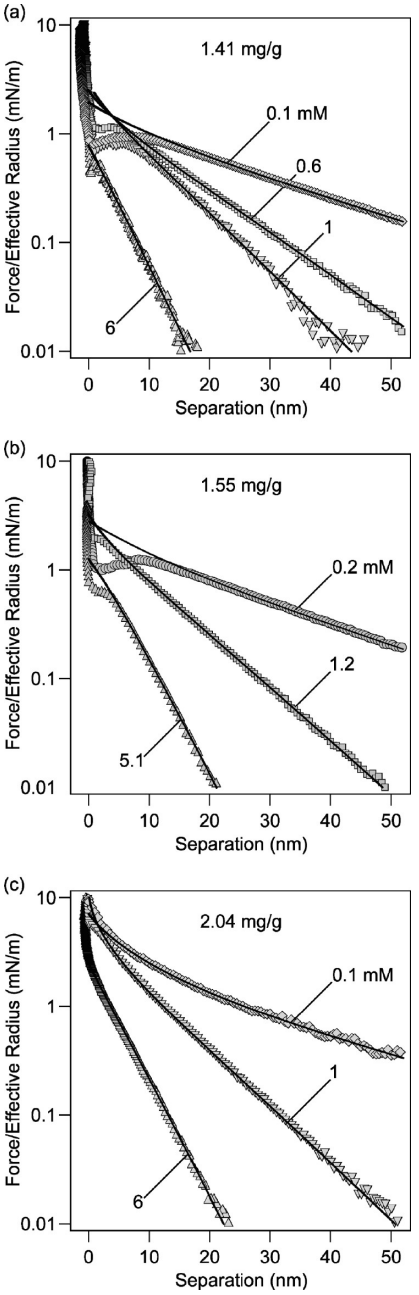

Figure 4. Interaction force profiles between sulfate latex particles with adsorbed PAMAM G10 dendrimer layers in KCl electrolyte at pH 4. The solid lines indicate fits with PB theory with CR boundary conditions. Adsorbed mass of dendrimers: (a) 1.41, (b) 1.55, and (c) 2.04 mg/g.

the ionic strength. The resulting charge densities are summarized in Table 1.

Interaction forces were equally studied at dendrimer doses below the saturation value. Under such conditions, the adsorption is quantitative and the adsorbed amount is limited by the dendrimer dose. The fact that all added dendrimers adsorb to the particles can be inferred from the surface number density, which is obtained by counting the individual adsorbed dendrimers with the AFM. When this quantity is compared to the amount of dendrimers added to the solution, the resulting values agree within experimental error.

Figure 6 shows the force profiles for dendrimer doses under such conditions at an ionic strength of 0.1 mM and

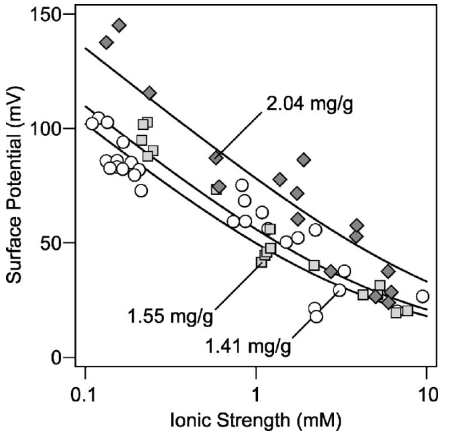

Figure 5. Measured diffuse layer potentials of latex particles with adsorbed PAMAM G10 dendrimers obtained from the force profiles as a function of ionic strength for different adsorbed masses. The solid lines are fits to the Gouy−Chapman relation. The resulting charge densities are given in Table 1.

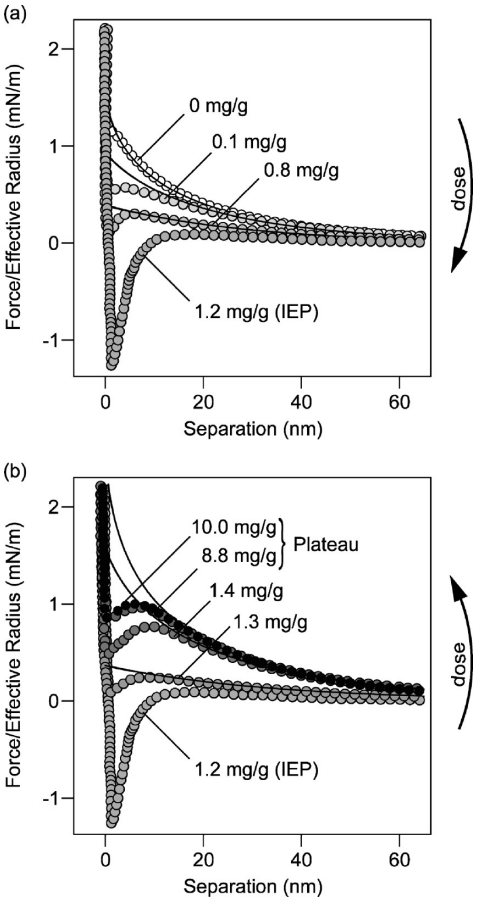

Figure 6. Interaction force profiles between sulfate latex particles with different added dose of PAMAM G10 dendrimer in 0.1 mM ionic strength. The solid lines are fits to the PB theory with CR boundary condition. The resulting charge densities are given in Figure 7: (a) below and at IEP; (b) at and above IEP.

pH 4. Recall that the forces between the bare latex particles in the absence of dendrimers are strongly repulsive due to diffuse layer overlap. With increasing dendrimer dose, the strength of the repulsion decreases until the force becomes attractive at a dose of 1.2 mg/g. This dose corresponds to vanishing electrophoretic mobility, which is referred to as the isoelectric point (IEP). When the dose is increased further,

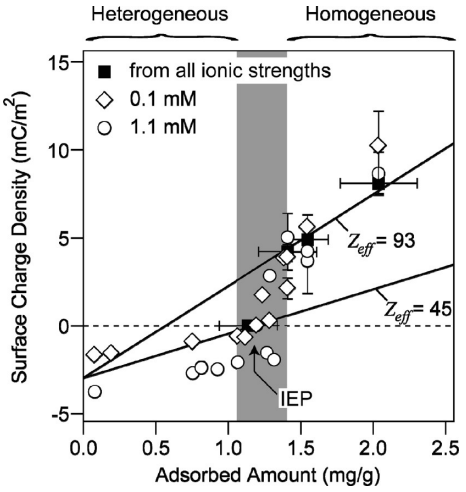

Figure 7. Surface charge compensating the diffuse layer charge as a function of the adsorbed density of latex particles. The solid lines represent the effective charges of 45 and 93 according to eq 3. The gray area indicates the transition between the homogeneous and heterogeneous region.

the force becomes repulsive again due to buildup of positive charge. At a dose of 1.4 mg/g, the saturation threshold is reached and the force remains constant even when the dose is increased beyond this point.

The observed forces are again dominated by repulsions due to diffuse layer overlap at larger distances. Attractive forces appear at shorter distances, and they are most prominent near the IEP. We suspect that these forces originate from patch-charge interactions.[41] The repulsive force profiles were fitted to the PB model. The decay length agrees well with the expected value from the solution composition, and the regulation parameters are $p = 0.18 \pm 0.05$ and 0.43 ± 0.03 at the ionic strengths of 0.1 mM and 1.1 mM, respectively. The resulting diffuse layer potential was converted to the corresponding surface charge density with the Gouy−Chapman relation (eq 2). The resulting surface charge density is shown as a function of the adsorbed amount in Figure 7. Surface charge densities obtained for the saturated adsorbed layers are equally included.

Effective Charge of Adsorbed Dendrimers. The surface charge compensating the charge of the diffuse layer can be used to evaluate the effective charge of the dendrimers in the adsorbed state. This overall surface charge density can be written as the sum of the surface charge of the bare particle and the contribution of the adsorbed dendrimers[37]

$$\sigma = \sigma_0 + eZ_{\text{eff}}\Gamma \tag{3}$$

where $\sigma_0 \simeq -3.0$ mC/m^2 is the surface charge of the bare particles as measured with the AFM, Z_{eff} is the effective charge expressed in units of the elementary charge e, and Γ the number density of the adsorbed dendrimers.

Figure 6 shows that the data for the saturated layers are well described with this relation, leading to an effective charge of $Z_{\text{eff}} = 93 \pm 4$. This value increases slightly with the ionic strength. However, below the IEP the increase is much more gradual, suggesting equally a linear relation, albeit with a smaller slope. The charge density rises sharply above the IEP. The more gradual increase prior to the IEP can be quantified by evaluating the effective charge from the position of the IEP. At this point, one has $\sigma = 0$, and therefore the effective charge can be expressed as

$$Z_{\text{eff}} = -\frac{\sigma_0}{e\Gamma_{\text{IEP}}} \tag{4}$$

where Γ_{IEP} is the adsorbed number density at IEP. This relation leads to a smaller effective charge of $Z_{\text{eff}} \simeq 45$. Table 2 summarizes these values.

Table 2. Effective Charges of Adsorbed Dendrimers

ionic strength[a] (mM)	saturated layer (expt)	IEP (expt)	PB[b] (theor)
0.1	90	45	64
1.1	91	45	83
10.1	97	45	139

[a] Ionic strength during the adsorption process. [b] Calculated with eq 5 for the ionic strength indicated.

The effective charges from experiment can be compared with the corresponding estimates based on PB theory. This theory predicts that the effective charge of a highly charged spherical object in an electrolyte solution will not exceed the value[39,40]

$$Z_{\text{eff}} = \frac{\tilde{a}}{L_{\text{B}}}(4\kappa\tilde{a} + 6) \tag{5}$$

where $\tilde{a}$ is the radius of the charged sphere and $L_{\text{B}} = e^2/(4\pi\varepsilon\varepsilon_0 kT) \simeq 0.72$ nm is the Bjerrum length evaluated at room temperature in water. Taking the solution radius of 6.7 nm of PAMAM G10 dendrimer, one obtains effective charges around 100 (see Table 2). These values are well comparable to the values for the effective charge observed for dendrimers in the saturated state. The fact that the effective charge of adsorbed dendrimers is somewhat different from the corresponding bulk value is not surprising. The reason for this discrepancy is that the diffuse layer around dendrimers adsorbed on a planar substrate is asymmetric, while it assumes a spherical symmetry in bulk. This point was previously demonstrated theoretically for charged particles adsorbed to air−water interfaces.[54]

The present findings can be related to similar results based on direct force measurements between saturated PAMAM dendrimer layers adsorbed at pH 4 to silica.[37] For G10 dendrimers, this study reports an effective charge of 53 ± 9. This value was also found to be relatively independent of the ionic strength, and is somewhat smaller than the presently reported value of about 93 ± 4 in the saturated state. The difference between these two values originates most likely from the different charges densities of the two substrates. The substrate in the mentioned study is silica,[37] and for the conditions investigated, its surface charge density is substantially smaller than the one of the latex particles here. This parameter was shown to influence the effective charge of colloidal particles at air−water interfaces.[54] However, similar studies for particles near a liquid−solid interface are lacking, and currently the importance of this effect is difficult to estimate. Moreover, the fact that PAMAM dendrimers flatten during adsorption to oppositely charged substrates complicates this aspect further.

At this point, we can only speculate why effective charges of adsorbed dendrimers are different in the two regimes mentioned. This transition could be related to changes in the structure of the diffuse layer around adsorbed dendrimers (see Figure 8). At low adsorbed amount, a diffuse layer develops around each individual dendrimer leading to a very heterogeneous charge distribution. This type of a diffuse layer leads to an optimal screening, and to the lowest value of

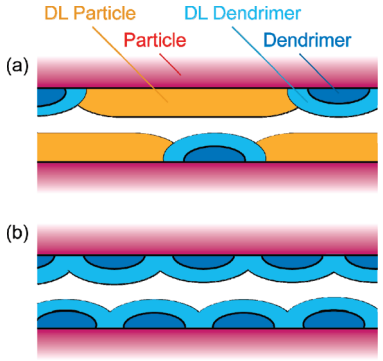

Figure 8. Scheme of the extent of the diffuse layers (DL) around the particle surface and adsorbed dendrimers: (a) heterogeneous regime at low adsorption density and (b) homogeneous regime at high adsorption density.

the effective charge. With increasing adsorbed amount, these diffuse layers start to overlap. When this overlap becomes noticeable, the adsorption process stops and leads to a saturated layer. However, when one exposes a saturated layer, which was formed at a higher ionic strength, to an electrolyte solution of a lower ionic strength, the diffuse layers will overlap even further. In this case of a more homogeneous layer, the dendrimers are screened less efficiently, leading to a higher value of the effective charge.

The effective charges reported in this article are somewhat lower than the values obtained with a model used in computer simulations of the same system.[41,55] The reason for these discrepancies is related to the fact that the latter model relies on screened Coulomb interactions between point charges, while smeared-out charge distributions are considered here.

4. Conclusions

Direct force measurements with the AFM were used to demonstrate that adsorbed cationic dendrimers lead to a charge reversal of negatively charged latex particles. Away from the IEP, the forces are dominated by diffuse layer repulsion. The magnitude of this repulsion is dictated by the compensating charge of the diffuse layer, which increases with increasing the adsorbed amount. A linear increase can be characterized by a constant effective charge of the dendrimer. However, two different regions are identified at low and high dendrimer dose. At low dose, the lateral surface charge distribution is highly heterogeneous and one finds a smaller effective charge. At high dose, the distribution is more homogeneous and a higher effective charge is obtained. The transition between these two regions is situated in a narrow region above the IEP, whereby the compensating charge increases very rapidly. We suspect that the transition is related to a transition in the extent of the diffuse layers around the adsorbed dendrimers (see Figure 8).

Acknowledgment. This research was supported by the Swiss National Science Foundation, University of Geneva, Swiss Federal Office for Education and Science, and COST Action D43.

References and Notes

(1) Borkovec, M.; Papastavrou, G. *Curr. Opin. Colloid Interface Sci.* **2008**, *13*, 429–437.
(2) *Retention aids*; 2nd ed.; Horn, D.; Linhart, F., Eds.; Blackie Academic and Professional: Glasgow, Scotland, 1996.
(3) Schwuger, M. J.; Subklew, G.; Woller, N. *Colloid Surf. A* **2001**, *186*, 229–242.
(4) Mezzenga, R.; Schurtenberger, P.; Burbidge, A.; Michel, M. *Nat. Mater.* **2005**, *4*, 729–740.
(5) de Gennes, P. G. *Nature* **2001**, *412*, 385–385.
(6) Russel, W. B.; Saville, D. A.; Schowalter, W. R. *Colloidal Dispersions*; Cambridge University Press: Cambridge, U.K., 1989.
(7) Gregory, J. *J. Colloid Interface Sci.* **1973**, *42*, 448–456.
(8) Bouyer, F.; Robben, A.; Yu, W. L.; Borkovec, M. *Langmuir* **2001**, *17*, 5225–5231.
(9) Ashmore, M.; Hearn, J.; Karpowicz, F. *Langmuir* **2001**, *17*, 1069–1073.
(10) Gillies, G.; Lin, W.; Borkovec, M. *J. Phys. Chem. B* **2007**, *111*, 8626–8633.
(11) Schwarz, S.; Jaeger, W.; Paulke, B. R.; Bratskaya, S.; Smolka, N.; Bohrisch, J. *J. Phys. Chem. B* **2007**, *111*, 8649–8654.
(12) Bauer, D.; Buchhammer, H.; Fuchs, A.; Jaeger, W.; Killmann, E.; Lunkwitz, K.; Rehmet, R.; Schwarz, S. *Colloids Surf. A* **1999**, *156*, 291–305.
(13) Verwey, E. J. W.; Overbeek, J. T. G. *Theory of Stability of Lyophobic Colloids*; Elsevier: Amsterdam, 1948.
(14) Derjaguin, B.; Landau, L. D. *Acta Phys. Chim.* **1941**, *14*, 633–662.
(15) Esumi, K.; Goino, M. *Langmuir* **1998**, *14*, 4466–4470.
(16) van Duijvenbode, R. C.; Koper, G. J. M.; Bohmer, M. R. *Langmuir* **2000**, *16*, 7713–7719.
(17) Lin, W.; Galletto, P.; Borkovec, M. *Langmuir* **2004**, *20*, 7465–7473.
(18) Sakai, K.; Sadayama, S.; Yoshimura, T.; Esumi, K. *J. Colloid Interface Sci.* **2002**, *254*, 406–409.
(19) Cahill, B. P.; Papastavrou, G.; Koper, G. J. M.; Borkovec, M. *Langmuir* **2008**, *24*, 465–473.
(20) Barnes, T. J.; Ametov, I.; Prestidge, C. A. *Langmuir* **2008**, *24*, 12398–12404.
(21) Kleijn, J. M.; Barten, D.; Cohen Stuart, M. A. *Langmuir* **2004**, *20*, 9703–9713.
(22) Longtin, R.; Maroni, P.; Borkovec, M. *Langmuir* **2009**, *25*, 2928–2934.
(23) Tomalia, D. A.; Baker, H.; Dewald, J.; Hall, M.; Kallos, G.; Martin, S.; Roeck, J.; Ryder, J.; Smith, P. *Macromolecules* **1986**, *19*, 2466–2468.
(24) Ballauff, M.; Likos, C. N. *Angew. Chem., Int. Ed.* **2004**, *43*, 2998–3020.
(25) Cakara, D.; Kleimann, J.; Borkovec, M. *Macromolecules* **2003**, *36*, 4201–4207.
(26) Fritzinger, B.; Scheler, U. *Macromol. Chem. Phys.* **2005**, *206*, 1288–1291.
(27) Prosa, T. J.; Bauer, B. J.; Amis, E. J. *Macromolecules* **2001**, *34*, 4897–4906.
(28) Betley, T. A.; Banaszak Holl, M. M.; Orr, B. G.; Swanson, D. R.; Tomalia, D. A.; Baker, J. R., Jr. *Langmuir* **2001**, *17*, 2768–2773.
(29) Pericet-Camara, R.; Papastavrou, G.; Borkovec, M. *Langmuir* **2004**, *20*, 3264–3270.
(30) Dahlgren, M. A. G.; Waltermo, A.; Blomberg, E.; Claesson, P. M.; Sjostrom, L.; Akesson, T.; Jonsson, B. *J. Phys. Chem.* **1993**, *97*, 11769–11775.
(31) Claesson, P. M.; Paulson, O. E. H.; Blomberg, E.; Burns, E. H. *Colloids Surf. A* **1997**, *123−124*, 341–353.
(32) Biggs, S.; Healy, T. W. *J. Chem. Soc. Faraday Trans.* **1994**, *90*, 3415–3421.
(33) Poptoshev, E.; Rutland, M. W.; Claesson, P. M. *Langmuir* **1999**, *15*, 7789–7794.
(34) Block, S.; Helm, C. A. *J. Phys. Chem. B* **2008**, *112*, 9318–9327.
(35) Pericet-Camara, R.; Papastavrou, G.; Behrens, S. H.; Helm, C. A.; Borkovec, M. *J. Colloid Interface Sci.* **2006**, *296*, 496–506.
(36) Kirwan, L. J.; Maroni, P.; Behrens, S. H.; Papastavrou, G.; Borkovec, M. *J. Phys. Chem. B* **2008**, *112*, 14609–14619.
(37) Pericet-Camara, R.; Papastavrou, G.; Borkovec, M. *Macromolecules* **2009**, *42*, 1749–1758.
(38) Buron, C. C.; Filiatre, C.; Membrey, F.; Perrot, H.; Foissy, A. *J. Colloid Interface Sci.* **2006**, *296*, 409–418.
(39) Chew, W. C.; Sen, P. S. *J. Chem. Phys.* **1982**, *77*, 2042–2044.
(40) Aubouy, M.; Trizac, E.; Bocquet, L. *J. Phys. A* **2003**, *36*, 5835–5840.
(41) Popa, I.; Papastavrou, G.; Borkovec, M.; Trulsson, M.; Jonsson, B. *Langmuir* **2009**, *25*, 12435–12438.
(42) Mansfield, M. L. *Macromolecules* **1993**, *26*, 3811–3814.
(43) Muller, R.; Laschober, C.; Szymanski, W. W.; Allmaier, G. *Macromolecules* **2007**, *40*, 5599–5605.
(44) Sader, J. E.; Larson, I.; Mulvaney, P.; White, L. R. *Rev. Sci. Instrum.* **1995**, *66*, 3789–3798.
(45) Cleveland, J. P.; Manne, S.; Bocek, D.; Hansma, P. K. *Rev. Sci. Instrum.* **1993**, *64*, 403–405.
(46) Hutter, J. L.; Bechhoefer, J. *Rev. Sci. Instrum.* **1993**, *64*, 1868–1873.
(47) Attard, P. *Adv. Colloid Interface Sci.* **2003**, *104*, 75–91.

(48) Zhang, X. H.; Quinn, A.; Ducker, W. A. *Langmuir* **2008**, *24*, 4756–4764.
(49) Pericet-Camara, R.; Papastavrou, G.; Behrens, S. H.; Borkovec, M. *J. Phys. Chem. B* **2004**, *108*, 19467–19475.
(50) Borkovec, M.; Behrens, S. H. *J. Phys. Chem. B* **2008**, *112*, 10795–10799.
(51) Mansfield, M. L. *Polymer* **1996**, *37*, 3835–3841.
(52) Mecke, A.; Lee, I.; Baker, J. R.; Holl, M. M. B.; Orr, B. G. *Eur. Phys. J. E* **2004**, *14*, 7–16.
(53) Miklavic, S. J. *J. Chem. Phys.* **1995**, *103*, 4794–4806.
(54) Frydel, D.; Dietrich, S.; Oettel, M. *Phys. Rev. Lett.* **2007**, *99*, 118302.
(55) Trulsson, M.; Forsman, J.; Akesson, T.; Jonsson, B. *Langmuir* **2009**, *25*, 6106–6112.